

# Force induced unfolding of bio-polymers in a cellular environment: A model study

Amit Raj Singh<sup>1</sup>, Debaprasad Giri<sup>2</sup>, and Sanjay Kumar<sup>1</sup>

<sup>1</sup>*Department of Physics, Banaras Hindu University, Varanasi 221 005, India*

<sup>2</sup>*Department of Applied Physics, IT, Banaras Hindu University, Varanasi 221 005, India*

(Dated: February 13, 2022)

Effect of molecular crowding and confinement experienced by protein in the cell during unfolding has been studied by modeling a linear polymer chain on a percolation cluster. It is known that internal structure of the cell changes in time, however, they do not change significantly from their initial structure. In order to model this we introduce the correlation among the different disorder realizations. It was shown that the force-extension behavior for correlated disorder in both constant force ensemble (CFE) and constant distance ensemble (CDE) is significantly different than the one obtained in absence of molecular crowding.

PACS numbers: 64.90.+b, 36.20.Ey, 82.35.Jk, 87.14.Gg

## I. INTRODUCTION

Understanding of the structure and function of bio-polymers in vivo by analyzing it in vitro is one approach [1, 2, 3, 4], but another route is to perform the analysis in presence of the environment similar to in vivo [5, 6, 7, 8]. It is now known that the interior of the cell contains different kind of biomolecules like sugar, nucleic acids, lipids etc. These macromolecules occupy about 40% of the total volume with steric repulsion among themselves. This confined environment induces phenomena like “molecular confinement” and “molecular crowding” and has major thermodynamic and kinetic consequences on the cellular processes [9, 10, 11]. In recent years, Single Molecule Force Spectroscopy (SMFS) experiments were mainly performed in vitro (absence of molecular crowding) to understand the cellular processes [1, 12, 13, 14]. Theoretical modeling of such processes with simplified interactions [15, 16, 17, 18, 19, 20, 21, 22, 23, 24] amenable to statistical mechanics have been used extensively to compare the outcomes of these experiments. Such models despite their simplicity, have been proved to be quite predictive and provided many important information about the cellular processes. In all such modeling, the confinement imposed by the cellular environment has been ignored and surrounding environment has been considered as homogeneous. For example in protein unfolding each amino acid (monomer) interacts with its fixed number (depending on the lattice) of nearest neighbors [19, 20, 21, 22, 23, 24].

In vivo, cellular environment and interactions involved in the stability of protein remain no more homogeneous. Hence in theoretical modeling, it is essential to use the underlying lattice to be disorder (or random) in order to study the effects of the cellular environment. If different biomolecules do not move with time the effect of such confinement is termed as “molecular confinement”. If they move, then effect is termed as “molecular crowding”. From the statistical mechanics perspective for the “molecular confinement”, quenched averaging is appropriate while for the “molecular crowding” constrained annealed averaging will be suitable. It is pertinent to mention here that unfolding process is a dynamical phenomenon of the order of micro seconds to few seconds. In such a short time span, internal structure of cell does not access all pos-

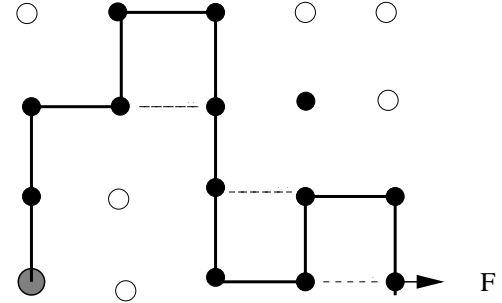


FIG. 1: Schematic representation of a polymer chain on a disordered lattice. The filled circle represents the available site and open circle represents the occupied sites. The imposed restriction of  $p_c$  above than the value 0.5928 represents the unavailability of fraction of sites (“volume exclusion” which is about 40% as seen in the cell). One end of the polymer chain is kept fixed while a force  $F$  has been applied at the other end.

require the averaging over all possible internal conformations ( $\rightarrow \infty$ ) of the the cell. Therefore, in present study, we restrict ourselves to finite, but a set of large disordered realizations which roughly reproduce the effect of the internal structure of the cell.

The aim of this paper is to study the effect of an applied force on a polymer trapped in a random environment as shown in Fig. 1. The random environment mimics the effect of crowding agents as seen in the cell. The confinement of the polymer to a restricted portion of phase space leads to the loss in entropy. Therefore, effect of the applied force on the reaction co-ordinate (in this case end to end distance) is mainly determined by the loss of configurational entropy and gain in internal energy because of the nearest neighbor interaction ( $\epsilon$ ). Because of the surrounding environment the average number of interactions per monomer is not constant, but may vary in between 0 to 2. This introduces heterogeneity in the interaction along the chain even in case of homopolymers. It is important to mention here that in this case the precise information about the reaction co-ordinate, probability distribution of the reaction co-ordinate on the parameters of the system is difficult to obtain analytically, therefore, one has to resort on numerical treatments.

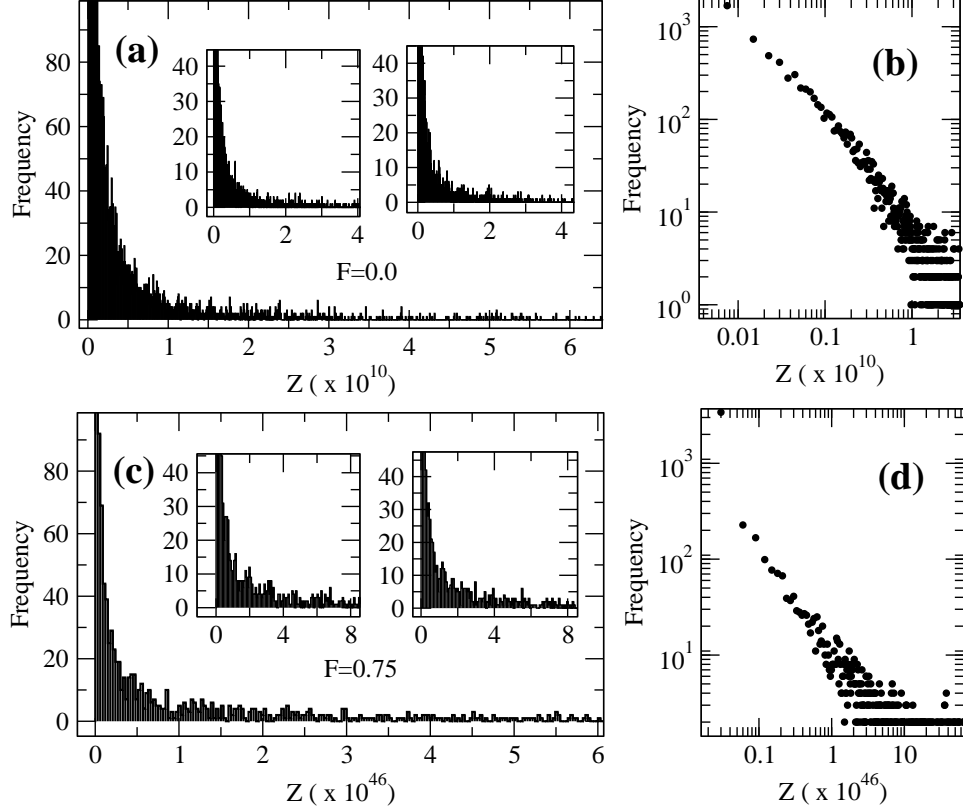


FIG. 2: (a) Histogram of  $Z$  at  $F = 0$  and  $T = \infty$ ; (b) Corresponding histogram in log-log scale shows the power law behavior; (c & d) Same as (a, b) but for  $F = .75$  and  $T = 0.3$ .

introduce the model to mimic the cellular environment and describe how we are considering the random correlated disorder environment. We also briefly discuss the exact enumeration technique in this section. In sec. III we present our main results obtained in constant force ensemble (CFE) and constant distance ensemble (CDE). We show the force-extension behavior in presence of crowding agents significantly different than the one obtained for the pure case which represents the unfolding process in vitro. We briefly discuss the consequence of molecular crowding and confinement in sec. IV.

## II. MODEL AND METHOD

### A. Random Environment: Correlated Disorder

We model a polymer chain described by the self attracting self avoiding walks (SASAWs) [16] confined in a random environment. Such environment can be obtained by using the method developed for the percolation cluster. We choose probability for an unoccupied site equal to  $p$  which is just above the percolation threshold  $p_c (= 0.5928)$  [25, 26, 27, 28]. This will offer a wide class of the distribution of clusters. Cluster size can vary from the isolated site to the length of the system. For the collapsed state the ground state energy arising due to the nearest neighbor interaction will not be constant. It can be stated that in case of random lattice, energy

state energy is  $-\epsilon N$  which is a constant.

Molecular crowding is a dynamical phenomenon involving the appearance, disappearance and movement of voids. Therefore, the internal structure of the cell changes continuously. Recently Singh et al [29] have studied the effect of molecular crowding by considering the underlying lattice as percolation cluster where each realization of disorder was independent of the previous disorder realization. In presence of molecular crowding agent, Yuan et al. [30] has performed the unfolding experiment for the first time. In order to model the cellular environment, they used dextran as crowding agents. From this experiment and from the knowledge accumulated from the structure of cell, it has been revealed that the internal structure of the cell changes over the time, but it does not change rapidly. Therefore, they consider the average effect of crowding agents on the unfolding. Hence their results do not distinguish between molecular confinement and molecular crowding. Since, the cell structures at different time stages remain correlated with the initial (native) structure, therefore, each realization should also be correlated with the initial (native) structure. In order to obtain the set of correlated percolation clusters, we choose a percolation cluster (native) and generate other clusters by changing certain fraction (in this case 10%) of the occupied site to unoccupied site and vice versa with respect to the native. This condition leads to a set of correlated percolation clusters, where each cluster is correlated with the native cluster but differs with each other with some

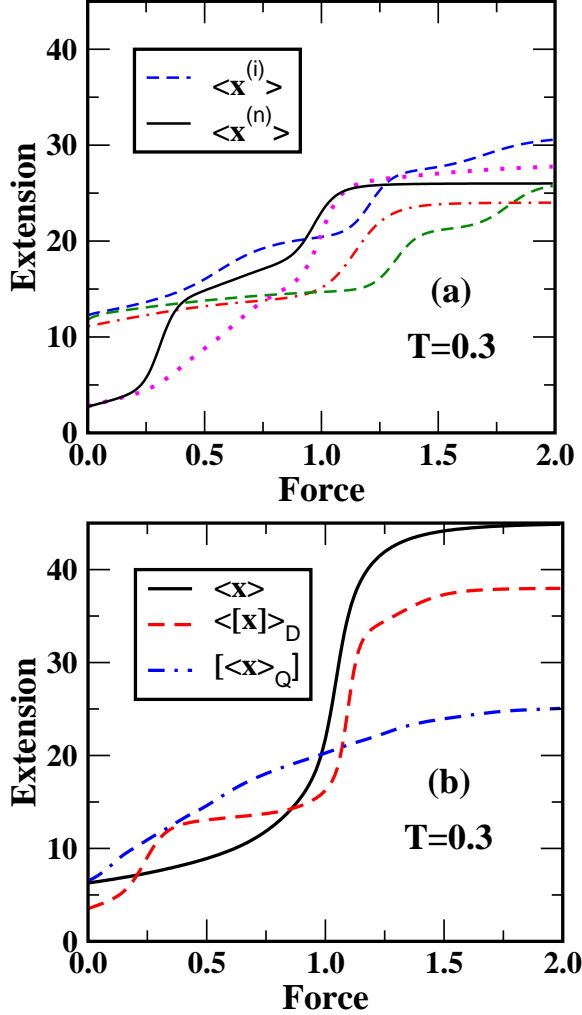


FIG. 3: Figures show the variation of reaction co-ordinate with force at different temperature in CFE: (a) Representative F-x curve for different disorder realizations at  $T=0.3$ .  $\langle x^{(n)} \rangle$  is for initial (native) realization and  $\langle x^{(i)} \rangle$  is for other realizations which differ from native by 10%; (b) F-x curve for approximate annealed average and sample averaged quenched disorder at temperature ( $T=0.3$ ); The native (initial realization), approximate annealed case and individual quenched disorder show the multi step plateaus which are absent in pure case.

order of correlation. This also ensures that the concentration of the crowding agent does not change, but the internal structure may change as happens in the cell. Since we are near to percolation threshold, every disorder realization constitute the partition function which is non zero. This will permit us to study the effect of cellular environment in a much more realistic

## B. Exact Enumeration Method

We enumerate all possible walks both on square lattice with disorder (percolation lattice) and without disorder (pure lattice). Since, all the single molecule experiments are of few monomers and hence the observed effect may have finite size effect. In this context exact enumeration technique has been proved to be quite successful in order to have better understanding of single molecule experiments of finite size. As the number of conformation increases with  $\mu^N$ , we restrict our calculation for chain length up to 45 steps walk. Here  $\mu$  is the connectivity constant of the lattice. The partition function of the  $i^{th}$  realization of the disorder configuration may be written as

$$Z^{(i)} = \sum_{(N_p, |x|)} C_N^{(i)}(N_p, |x|) u^{N_p} \omega^{|x|}. \quad (1)$$

Here  $C_N^{(i)}(N_p, |x|)$  is the number of distinct conformations of walks of length  $N$  in the  $i$ -th realization of the disorder with  $N_p$  non-bonded nearest neighbor pairs and whose end-points are a distance  $x$  apart.  $\omega (= \exp[\beta(\mathbf{F} \cdot \hat{x})])$  is the Boltzmann weight for the force, where  $\hat{x}$  is the unit vector along the  $x$ -axis and  $\beta$  is defined as  $\frac{1}{kT}$ . Here,  $k$  is the Boltzmann constant and  $T$  is the temperature.  $u (= \exp(-\beta\epsilon_u))$  is the Boltzmann weight for nearest neighbor interaction.

In the following, we set  $\epsilon/k = 1$  and focus our discussion on force-extension behavior in CFE and CDE. In the present study we consider 10000 realizations ( $N_{tot}$ ) of the correlated percolation clusters. In Fig. 2(a), we plot the histogram of  $Z$  for all 10000 realizations. It is surprising to see that each realization which differs from the native conformation by 10% only give such a wide range ( $10^3$  to  $10^{10}$ ) of the distribution of  $C_N$ . The existence of long tail in the distribution indicates that the standard deviation will be quite larger than the mean value. The log-normal distribution of the above histogram of 5000 realization shown in inset of Fig. 2a, give mean value  $\approx 18.2$  and standard deviation  $\approx 3.1$  for each set. In Fig. 2(b), we plot the frequency of  $Z$  with rank in the log-log scale. From this plot, we find power law behavior. In Fig. 2(c), we plot histogram at intermediate temperature and force ( $T = 0.3$  and  $F = 0.75$ ) and found that the qualitative behavior (long tail) of the histogram and the power law (Fig. 2(d)) remain the same.

## III. AVERAGING OVER DISORDER

Following the method developed in ref. [29] we denote a sample average over various realizations as  $[...]$  and thermal averaging as  $\langle ... \rangle$ .

### A. Force-Extension Behavior in CFE

In CFE, for a given realization of disorder, we calculate the reaction coordinate i.e  $x$ -component of end-to-end distance from the following expression

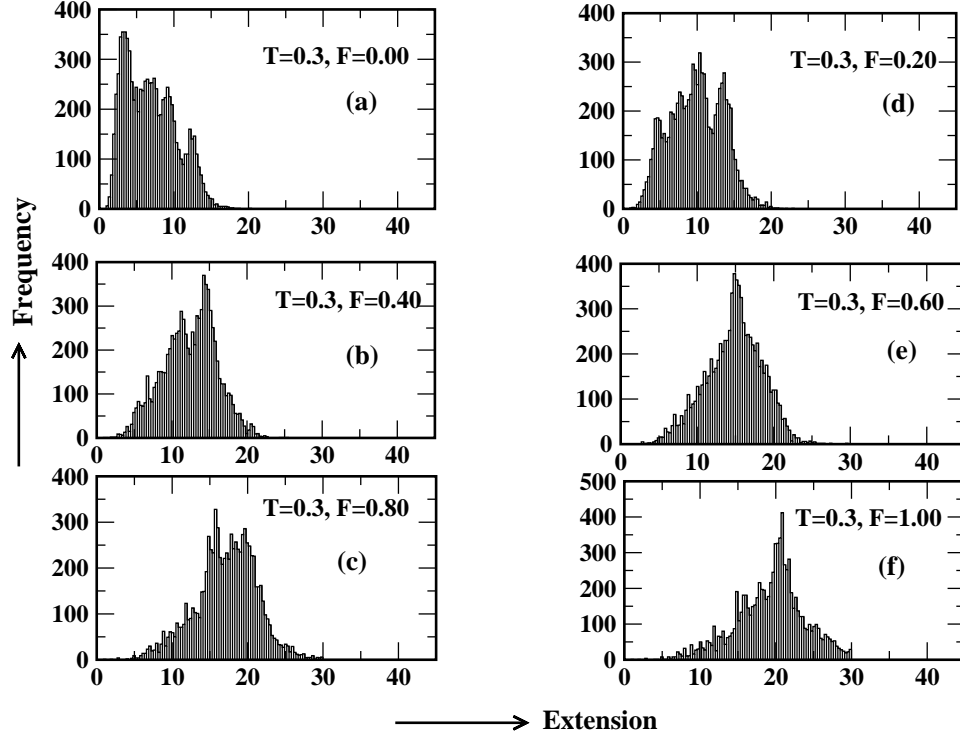


FIG. 4: Histogram of extension of various realizations at different forces and fixed temperature ( $T = 0.3$ ).

$$\langle x^{(i)} \rangle_Q = \frac{\sum_{(N_p, |x|)} x^{(i)} C_N^{(i)}(N_p, |x|) u^{N_p \omega |x|}}{Z^{(i)}} \quad (2)$$

This may be thought as simple representation of molecular confinement where disorder sites do not move with time. Therefore, we refer it as quenched average of  $i$ -th realization. The sample average over Eq. (2) can be written as

$$[\langle x \rangle_Q] = \sum_i \langle x^{(i)} \rangle_Q / N_{tot} \quad (3)$$

which we call the sample average over quenched disorder. In Fig. 3(a) we show some of the representative plots for different correlated realizations. The qualitative nature of  $F$ - $x$  curve almost remain same, but vary for different realizations. All these plots show the existence of plateaus. It may be noted that the number of plateaus may vary from realization to realization. The sample averaged reaction coordinate has also been shown in Fig. 3(b) at low temperature. As pointed above, because of large variation in the partition functions of different realizations, reaction coordinate also exhibits the similar variations. In Fig. 4, we plot the histogram of reaction coordinate for different realizations. With rise of force, the distribution peak shifts to the right. However, due to the large width of the histogram, the plateaus seen in individual realization

does not mean the plateau vanishes. In fact all these plateau exist for different realization. In Fig. 5a, we plot the probability distribution of plateaus ( $P(ip)$ ) at  $T = 0.3$ . The variation of sample average of number of plateaus ( $[ip]$ ) with temperature is shown in Fig. 5b. From these plots, it is evident that average number of plateaus decreases with temperature and system approaches to two-state at high temperature.

For molecular crowding, we average over finite but large number of realizations. The realization in the limit  $N_{tot} \rightarrow \infty$  is not an experimental requirement. Since, the correlated percolation clusters are having the structures close to the initial cluster, therefore, obtaining all possible percolation clusters are beyond the scope. Hence we call the averaging over finite correlated clusters as an approximate annealed average. It is important to mention here that this averaging will vary on the choice of initial cluster as well as on the number of realizations. Moreover because of long tail in the distribution, two different sets of realizations may not give exactly the similar  $F$ - $x$  curve. However, qualitative nature of the  $F$ - $x$  curve for two different sets will remain same. The reaction coordinate (end-to-end distance) in case of approximate annealed averaging has been defined as

$$[\langle x \rangle]_D = \frac{\frac{1}{N_{tot}} \sum_i \sum_{(N_p, |x|)} x^{(i)} C_N^{(i)}(N_p, |x|) u^{N_p \omega |x|}}{Z} \quad (4)$$

realizations of the disorder. Though in the limit  $N_{tot} \rightarrow \infty$ , annealed average and pure give the same result, however, in present case this may not be true. Because all the correlated percolation clusters are having the structures close to the initial cluster and hence all possible conformations of disorder are not possible to generate. In Fig. 3b, we also plot the force extension curve for the approximate annealed case which also shows the existence of plateaus / intermediate states. At  $T = 0.3$ , we find two plateaus (Fig. 3b) which is close to the average number of plateaus ( $[ip]$ ) obtained by sample averaged quenched case (Fig. 5b).

### B. Force-Extension Behavior in CDE

It is known that atomic force microscopy (AFM) experiments work on CDE. When the disorder realizations were independent to each other Singh et.al. [29] have shown strong oscillations in F-x curve in CDE for approximate annealed case. Surprisingly such oscillations were absent for pure (in absence of disorder) and sample averaged quenched disorder.

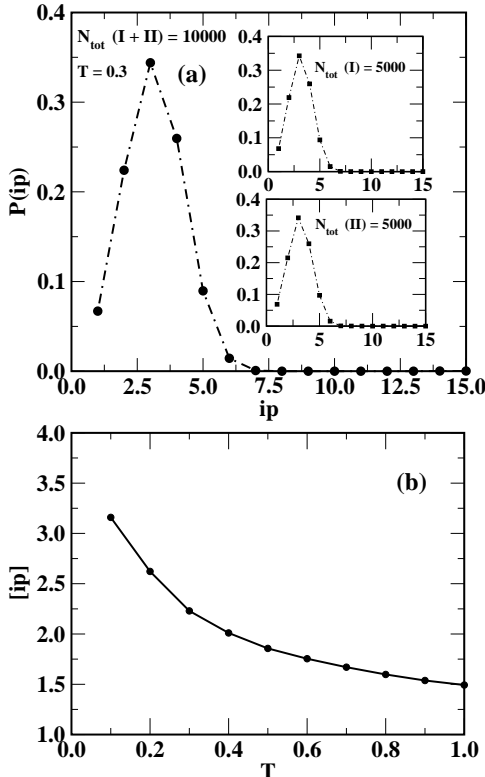


FIG. 5: (a) Probability of average number of plateaus at fixed temperature ( $T = 0.3$ ) for 10000 disorder realizations. Insets show the same plot for two different 5000 disorder realizations. All these normalized plot of probability overlaps with each other; (b) Plot of average number of plateaus ( $[ip]$ ) with temperature for sample averaged quenched case.

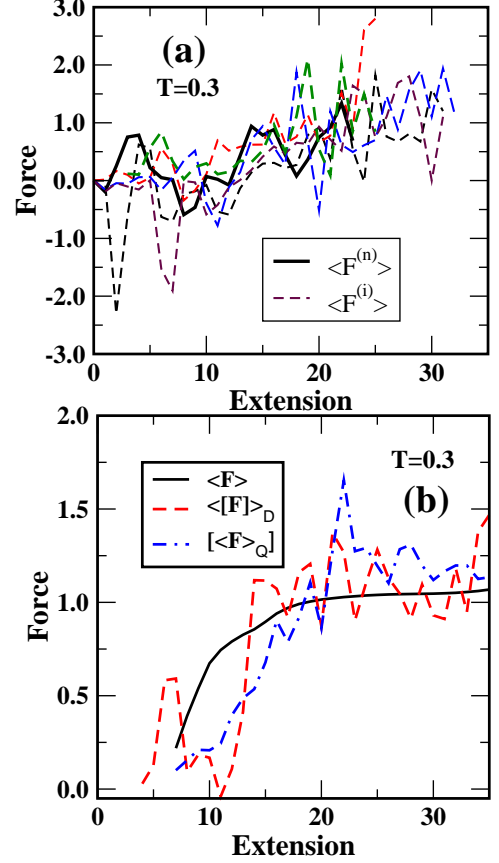


FIG. 6: Same as Fig. 3, but at CDE for temperature  $T = 0.3$ .

In present case where each realization is correlated, we observe strong oscillations (Fig. 6) in both approximate annealed and sample averaged quenched cases. This may be because in CDE the system probes local ground state energy which may be quite close for each disorder realization. However in case of independent realizations local ground state energy will be different for each realization and hence sample averaging will smoothen out such oscillations.

### C. Probability Distribution

In Fig 7 and 8, we show the probability distribution curves of reaction coordinate for different forces at fixed temperature. This provides important information about the changes in the structural processes in cellular environment. In our calculation we use the following expressions to calculate probability distribution for the approximate annealed and sample averaged quenched cases:

$$P_A(x) = \frac{\sum_i \sum_{N_P} C_N^{(i)}(N_P, |x|) u^{N_P \omega |x|}}{\sum_i Z^{(i)}} \quad (5)$$

and

$$P_Q(x) = \frac{1}{N_{\text{tot}}} \sum_i \left[ \frac{\sum_{N_P} C_N^{(i)}(N_P, |x|) u^{N_P \omega |x|}}{Z^{(i)}} \right] \quad (6)$$

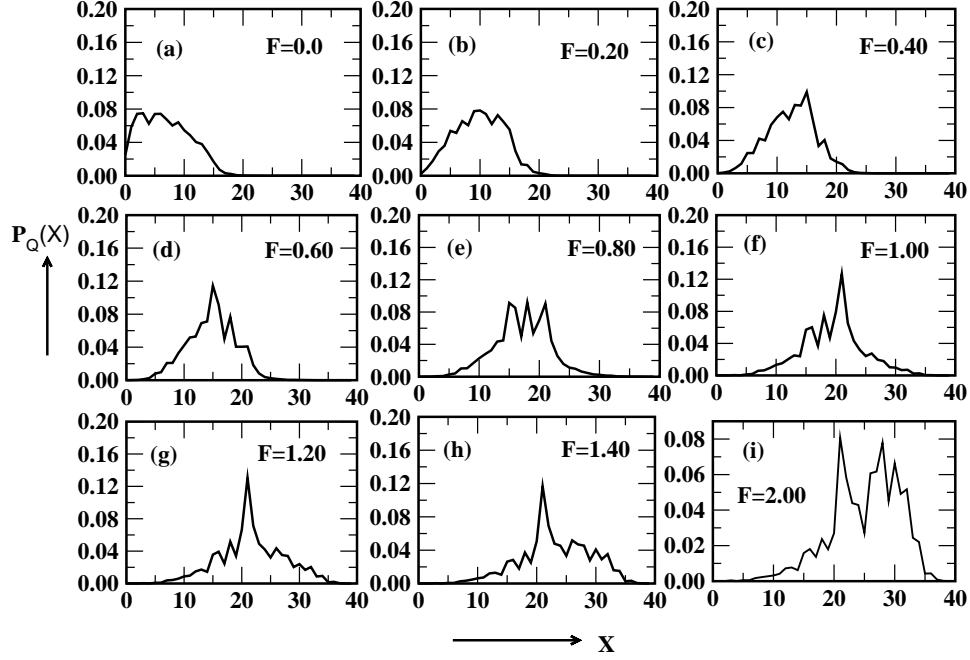


FIG. 7: Plot of  $P(x)$  vs  $x$  for sample averaged quenched disorder case at different  $F$  (fixed temperature  $T = 0.3$ ).

For pure case the probability distribution curve has been studied by Singh et. al. [29]. For the correlated disorder we find qualitatively similar behaviour at lower and higher forces. At low force, the peak in the probability distribution corresponds to the collapsed state and at high force it corresponds to the stretched state. It was found that for the pure case at certain force (near the transition point) the peak broadens which indicates that the transition is continuous. However, for the correlated disorder case (for both approximate annealed and sample averaged quenched disorder), one can see the emergence and disappearance of peaks [Fig 7 and 8] for different  $F$  at  $T = 0.3$ . In case of sample averaged quenched case the probability distribution profile is broad in nature with many small sharp peaks [Fig. 7]. Since entropy associated with sample averaged quenched disorder is much higher, therefore, the width of the peak broadens. However, for approximate annealed case the width of the peak remains smaller which is evident from Fig. 8. With increasing force, we see the height of one peak increases while others decreases. We find at many different forces the height of two peaks (at different position) become equal indicating the existence of two states. Unlike pure case, this reflects that disorder may change the order of transition and there will be emergence of intermediate states which are solely induced by the disorder.

#### IV. CONCLUSIONS

We have studied the effect of an applied force on globule-

mented here clearly shows that force induced transition as observed in vitro is quite different than in vivo. It is evident from our model studies that molecular crowding or molecular confinement induces intermediate states which may be seen in the form of plateaus in  $F$ - $x$  curve at CFE. It is interesting to note that quenched average over different disorder also show the existence of intermediate states similar to approximate annealed case. Because of the heterogeneity in the number of non-bonded nearest neighbor interaction (number may vary in between 0 to 2) along the chain and the structure of disorder, we see oscillations in  $F$ - $x$  curve in CDE for both approximate annealed and sample averaged quenched cases which were found to be absent for the uncorrelated disorder [29].

There are many biological events which are rare in nature. The occurrence of such event may be because of long-tail behavior in the distribution of partition function. Therefore, at this moment of time additional numerical and experimental works are required to understand the effect of crowding agents on unfolding processes seen in the cell.

#### V. ACKNOWLEDGMENT

We thank Department of Science and Technology and University Grants Commission, New Delhi for financial support. We acknowledge the generous computers support from

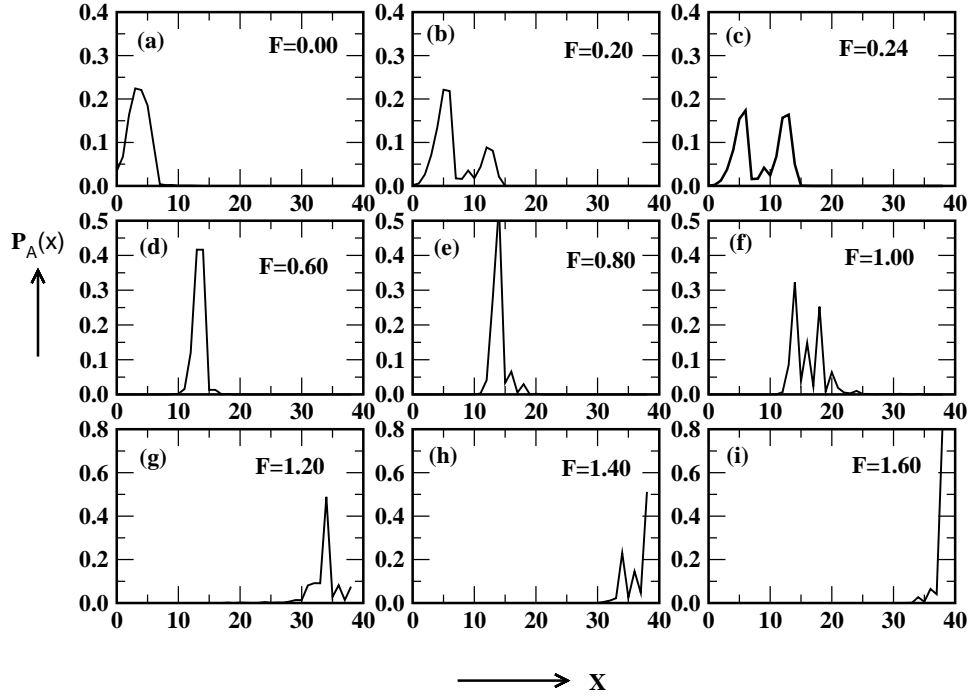


FIG. 8: Same as Fig. 7, but for the approximate annealed average case at different  $F$  (fixed temperature  $T = 0.3$ ).

- 
- [1] M. Rief *et al.*, *Science* **276**, 1109 (1997).
  - [2] M. S. Z. Kellermayer *et al.*, *Science* **276**, 1112 (1997); L. Tskhovrebova *et al.*, *Nature* **387**, 308 (1997).
  - [3] L. S. Itzhaki and P. A. Evans, *Protein Sci.* **5**, 140 (1996).
  - [4] A. S. Lemak, J. R. Lepock and J. Z. Y. Chen, *Phys. Rev. E* **67**, 031910 (2003); A. S. Lemak, J. R. Lepock and J. Z. Y. Chen, *Proteins: Structures, Function and Genetics* **51**, 224 (2003).
  - [5] R. J. Ellis and F. U. Hartl, *Curr. Opin. Struc. Biol.* **9**, 102 (1999)
  - [6] A. Matouschek, *Curr. Opin Struc. Biol.* **13**, 98 (2003).
  - [7] D. S. Goodesell, *Trends Bichem. Sci.* **16**, 203 (1991); A. E. Johnson, *Biochemical Society Transactions*, **32**, 668 (2004); A. Horwich, *Nature* **431**, 520 (2004).
  - [8] D. J. Mueller and Y. F. Dufrene, *Nature Nanotechnology*, **3**, 261 (2008).
  - [9] A. P. Minton, *J. Biol. Chem.* **276** 10577 (2001); A. P. Minton, *Curr. Opin. Struc. Biol.* **10** 34, (2000); R. J. Ellis, *Trend Biochem. Sci* **26**, 597 (2001).
  - [10] M. S. Cheung, D. Klinov and D. Thirumalai, *PNAS* **102**, 4753 (2005); L. Stagg *et al.*, *PNAS* **104**, 18976 (2007).
  - [11]
  - [12] M. Rief *et al.*, *Science* **275**, 1295 (1997).
  - [13] S. B. Smith, Y. Cui and C. Bustamante *Science* **271**, 795 (1996).
  - [14] C. Bustamante, Z. Bryant and S. B. Smith, *Nature* **42**, 423 (2003).
  - [15] M. Fixman, *J. Chem. Phys.* **58**, 1559 (1973).
  - [16] P. G. de Gennes *Scaling Concepts in Polymer Physics* (Cornell University press:Ithaca, 1979).
  - [17] M. Doi and S. F. Edwards, *Theory of Polymer Dynamics* (Oxford University Press: Oxford, 1986).
  - [18] C. Vanderzande, *Lattice Models of Polymers* (Cambridge University Press: Cambridge, 1998).
  - [19] M. S. Li *et al.*, *Biophys. J.* **92**, 547 (2007); M. S. Li, *Biophys. J.* **93**, 2644 (2007).
  - [20] R. Kapri and S. M. Bhattacharjee *Phys. Rev. Lett.* **98**, 098101 (2007); R. Kapri, S. M. Bhattacharjee and F. Seno, *Phys. Rev. Lett.* **93**, 248102 (2004).
  - [21] D. Marenduzzo *et al.* *Phys. Rev. Lett* **88**, 028102 (2002);
  - [22] D. Marenduzzo, *et al.* *Phys. Rev. Lett.* **90**, 088301 (2003).
  - [23] S. Kumar and D. Giri, *Phys. Rev. E* **72**, 052901 (2005).
  - [24] H.J. Zhou *et al.* *Phys. Rev. Lett.* **97**, 158302 (2007).
  - [25] B. K. Charabarti, *Statistics of Linear Polymers in Disordered Media*, (Elsevier, Amsterdam, 2005).
  - [26] K. Barat, S. N. Karamakar and B. K. Chakraborty, *J. Phys. A* **24**, 851 (1991), K. Barat and B. K. Chakraborty, *Physics Reports* **258**, 377 (1995).
  - [27] V. Blavatska and W. Janke, *Europhys. Lett.* **82**, 66006 (2008).
  - [28] D. Stauffer and A. Aharony, *Introduction to Percolation Theory*, (Taylor and Francis: London 1992).
  - [29] A. R. Singh, D. Giri and S. Kumar, *Phys. Rev. E* **79**, xxxxx (2009).
  - [30] J-M. Yuan *et al.* *Protein Sci.* **17**, 2156 (2008); 0:ps.037325.108v1-ps.037325.108.